An investigation of perpendicularly across twin-tunnel interaction

T. Boonyarak & C.W.W. Ng
The Hong Kong University of Science and Technology, HKSAR

D. Mašín
Charles University in Prague, Czech Republic

ABSTRACT: Any tunnel driving inevitably induces stress changes and deformation in the ground as well as adjacent substructures such as existing tunnels. Due to the shortage of lands and environmental needs in major cities worldwide, tunnels are constructed closer and closer. The interaction between tunnels is complex and still not fully understood. In this study, a three-dimensional centrifuge test was carried out to investigate the interaction between an existing tunnel and a new tunnel excavated perpendicularly across underneath in sand. A novel technique that simulates the effects of both volume and weight losses due to tunnel excavation has been recently developed to mimic three-dimensional effects of tunnel advancement in-flight. The test was also back-analyzed three-dimensionally using a non-linear constitutive model considering small strain stiffness. Interpretations of measured and computed results are reported and discussed.

1 INTRODUCTION

An increasing number of constructed tunnels in urban area causes the clear distance between tunnels to become smaller and smaller. As a result, excessive deformation and cracks on an existing tunnel may be induced by a new tunnel driving closely across underneath.

Large differential tunnel settlement along with cracks observed on the lining of existing tunnels caused by the excavation of new tunnels underneath was reported (Cooper et al., 2002; Li & Yuan, 2012).

Physical model tests at 1g conditions of cross tunnels in clay were illustrated by Kim et al. (1998). Tunneling was simulated by using a model shield machine. They reported that vertical compression of the existing tunnel due to large jacking force was observed.

Vorster et al. (2005) adopted the technique to simulate tunneling in centrifuge by controlling water extraction from annulus fitted around a hollow mandrel. The tunneling process was carried out in plane strain condition to study the effects of tunneling on pipelines in sand.

Verruijt & Strack (2008) investigated the effects of soil removal inside the tunnel by using plane strain numerical analysis with an elastic soil model. They suggested that effects of weight loss due to removal of soil inside the tunnel cause smaller and narrower ground surface settlement.

Liu et al. (2009) study the cross-tunnel interaction by using three-dimensional numerical analysis. They found that the interaction between perpendicularly crossing tunnels during tunnel advancing process was larger than those at the end of tunnel excavation.

In order to overcome the limitations of modeling tunnel excavation under the plane strain conditions, Ng et al. (2013) simulated three-dimensional tunnel advancement in centrifuge. In-flight tunnel excavation was simulated by considering both effects of volume and weight losses using a newly developed "donut". Comparisons were made between tests with and without mimicking weight loss due to tunnel advancement in centrifuge. In their paper, they investigated the effects of a new tunnel advancement at cover (C) to tunnel diameter (D) ratio (i.e. C/D) of 3.5 on an existing tunnel located at C/D of 2.0.

In this paper, a three-dimensional centrifuge test carried out to study perpendicularly cross-tunnel interaction in sand is reported. Different from the tests reported by Ng et al. (2013), a new tunnel excavated at C/D of 5.0 underneath an existing tunnel located at C/D of 3.5 is investigated in this current study. To verify test results and to improve our fundamental understanding of cross-tunnel interaction, three-dimensional numerical back-analysis performed is also described and reported.

2 THREE-DIMENSIONAL CENTRIFUGE TEST

2.1 *Centrifuge model package and model preparation*

Figure 1 shows a plan view of three-dimensional centrifuge model package of perpendicularly cross-

ing tunnels. Both existing and new tunnel has an outside diameter of 6 m in prototype. Totally six-stage tunnel advancement was conducted in-flight. The length of each excavation stage was equivalent to 3.6 m in prototype or 0.6D (where D is tunnel diameter). Reference axes, the "X" axis and the "Y" axis, refer to the longitudinal and transverse directions of the existing tunnel, respectively.

Figure 1b shows an elevation view of the centrifuge model package. The cover depth of the existing tunnel and pillar depth (i.e. clear distance between the existing and the new tunnel) was equivalent to 21 and 3 m, respectively in prototype. By normalizing with tunnel diameter (D), the cover-to-diameter ratio (C/D) of the existing tunnel and the pillar-to-diameter ratio (P/D) was 3.5 and 0.5, respectively.

The model tunnel was made of hollow aluminum alloy tube with a lining thickness of 3 mm in model scale. The tunnel lining was converted into equivalent thickness of concrete by assuming that the compressive strength of concrete (f'_c) was 50 MPa. As a result, Young's modulus of concrete (E_c) was estimated to be 33 GPa (ACI318M, 2011). The prototype tunnel lining thicknesses were thus equivalent to 230 and 420 mm in the transverse and longitudinal directions of each tunnel, respectively.

The new tunnel advancement was simulated three-dimensionally in-flight by using six "Donuts" (refers to Fig. 2). Each "Donut" was made of two pairs of rubber membranes. The outer rubber membrane covered around the tunnel lining while the inner one was encased in the tunnel lining. During the model preparation, heavy fluid (i.e. $ZnCl_2$) having a density of 1500 kg/m^3 was injected into both rubber membranes. The outer rubber membrane simulates the effects of volume loss, which is equivalent to 2% in this study. The inner rubber membrane mimics the effects of soil removal inside the tunnel or so-called effects of weight loss. More details are given by Ng et al. (2013).

Dry Toyoura sand was adopted in this study because a ratio between the model tunnels and the particle size (Ishihara, 1993) was about 500. Garnier et al. (2007) suggested that the grained size effects on soil-structure interaction was not significant when the ratio of tunnel diameter to average particle size was larger than 175. The dry density of 1529 kg/m^3 or equivalent to relative density of 64% was achieved by dry pluviation technique.

2.2 *Instrumentation*

Instrumentation used in the centrifuge test consisted of LVDTs and transverse bending moment transducers (Fig. 1b). Ground surface settlement was measured by three LVDTs installed at an offset distance of 0, 0.5D and 1.5D away from the new tunnel centerline. Tunnel settlement was measured by LVDTs connected to three extension rods mounted along the crown of the existing tunnel. The three extension rods were located at an offset distance of 0.5D, 1.5D and 3D away from the new tunnel centerline.

At the location directly above the new tunnel, eight transverse bending moment transducers were mounted on both sides of the existing tunnel lining. Each transverse bending moment transducer was evenly installed at 45 degrees around the circumference of the existing tunnel. In order to compensate for temperature effects, the transverse bending moment transducer was made of full Wheatstone bridge strain gauges.

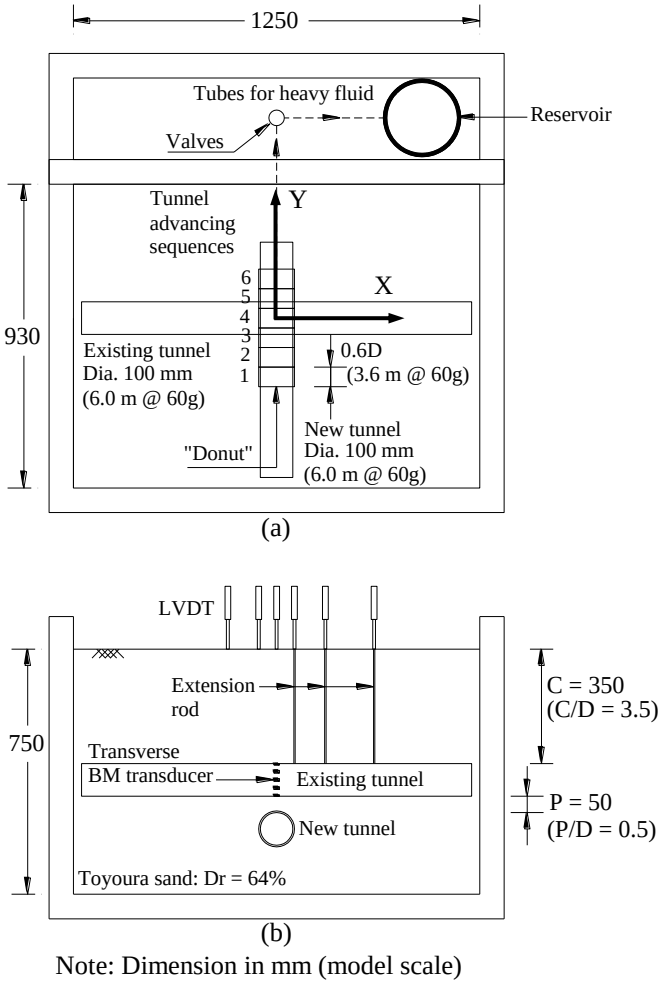

Note: Dimension in mm (model scale)

Figure 1. Schematic diagram showing a centrifuge model package for simulating effects of perpendicularly crossing-tunnel interaction: (a) plan; (b) elevation.

2.3 *Test procedures*

The test was carried out in a geotechnical centrifuge located at the Hong Kong University of Science & Technology (Ng et al., 2001, 2002). First, the model package was prepared and then moved to the centrifuge platform. After the LVDTs and transducers were calibrated, the centrifugal acceleration was increased to 60g. The initial reading was taken after there was no further change of reading from each transducer when the centrifugal acceleration reached 60g. Then tunnel advancement was carried out by draining away heavy fluid from each "Donut" one after another until reached the sixth excavation stage

(see Fig. 1a). After the completion of tunnel advancement, the centrifuge was spun down to 1g.

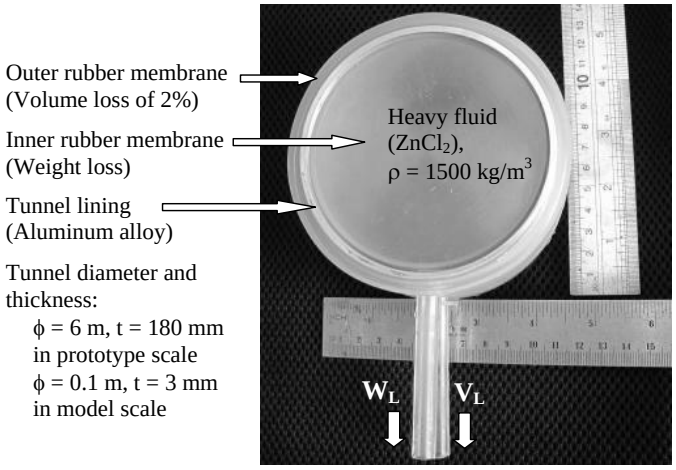

Figure 2. A "donut" for simulating effects of volume and weight losses during tunnel advancement (after Ng et al., 2013).

3 THREE-DIMENSIONAL NUMERICAL BACK-ANALYSIS

3.1 *Finite element mesh and boundary conditions*

Figure 3 shows the finite element mesh used to back-analyze the centrifuge test result in this study. Numerical analysis was carried out by using a commercial finite element program PLAXIS 3D 2012 (Brinkgreve et al., 2012). The dimension of the mesh was identical to that in the centrifuge test. Due to symmetry, only half of the whole model was simulated in numerical analyses by specifying the plane of symmetry boundary condition at X/D = 0. The boundary conditions of the other three vertical sides were roller support while hinge support was applied to the bottom boundary.

3.2 *Constitutive model and model parameters*

In this study, a hypoplastic constitutive model with intergranular strain concept was adopted to model dry Toyoura sand. The constitutive models have been developed to describe the non-linear response of granular material (Kolymbas, 1991; Gudehus, 1996; von Wolffersdorff, 1996; Wu et al., 1996). Intergranular strain concept or small strain stiffness considering stiffness dependency on strain and recent stress history is incorporated in the model by Niemunis & Herle (1997).

Model parameters were adopted from literature related to testing of Toyoura sand (Herle & Gudehus, 1999; Yamashita et al., 2000). At-rest earth pressure coefficient (K_0) was assumed to be 0.5. The tunnel lining was modeled as a shell element linear elastic material with a Young's modulus of 69 GPa. Density and Poisson's ratio of the tunnel lining were assumed to be 2700 kg/m^3 and 0.33, respectively. Model parameters adopted in this study were summarized in Table 1.

3.3 *Numerical analysis procedures*

The numerical analysis procedures basically followed that in centrifuge test. At the initial stage in 1g conditions, the soil inside the existing tunnel and some part of soil inside the new tunnel was removed. In order to simulate the effects of centrifugal acceleration increase, unit weight of both soil and tunnel were increased by 60 times. Then, tunnel excavation in each stage was carried out by simulating the effects of both volume and weight losses. The effects of volume loss, which was equivalent to 2%, were simulated by contracting the cylindrical surface around the tunnel lining by using a "surface contraction" function. The effects of weight loss were simulated by removing the soil inside each excavated section of the new tunnel.

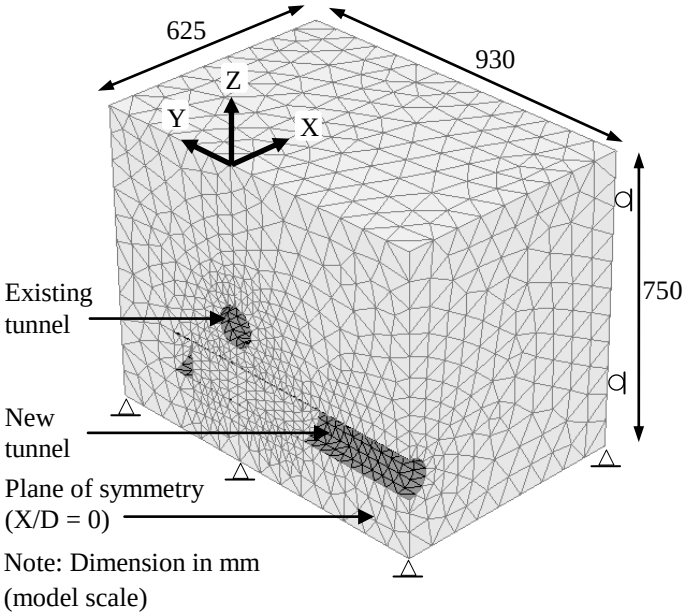

Figure 3. Finite element mesh and boundary conditions.

Table 1. Summary of model parameters adopted for finite element analysis.

Basic model parameters		Intergranular strain parameters	
ϕ_c	30	m_R	8
h_s	2.6 GPa	m_T	4
n	0.27	R	0.00002
e_{d0}	0.61	β_r	0.05
e_{c0}	0.98	χ	3.5
e_{i0}	1.10		
α	0.14		
β	3.0		

4 INTERPRETATION OF RESULTS

Measured and computed results reported in this paper are in prototype scale unless otherwise stated.

4.1 *Existing tunnel settlement*

Figure 4 shows comparison of measured and computed existing tunnel settlement. The tunnel settlement was normalized by each tunnel diameter. The maximum measured tunnel settlement was about

0.3%D or 18 mm, which exceeded the allowable limit of 15 mm recommended by LTA (2000). In addition, the maximum measured gradient reached the allowable limit of 1:1000 recommended by both LTA and BD. The computed results overestimated the measured results by about 15%, but the overall trend reasonably captured major aspects of the measured results.

The measured existing tunnel settlement in this study was compared with two case histories. Triple tunnels excavation underneath twin existing tunnel in London Clay was reported by Cooper et al. (2002). The tunnels were constructed by pilot shield tunnel with shield enlargement resulting in about 2.5% volume loss. Li & Yuan (2012) illustrated a case study of twin EPB shield tunnel underneath an existing double deck tunnel in Shenzhen highly decomposed granite.

By considering the flexural stiffness (EI) of the existing tunnel between the three cases, the existing tunnel EI in Cooper et al. (2002) was the smallest, while the existing tunnel EI in Li & Yuan (2012) was the largest. It is as expected that the largest existing tunnel settlement and tunnel gradient should occur in Cooper et al. (2002).

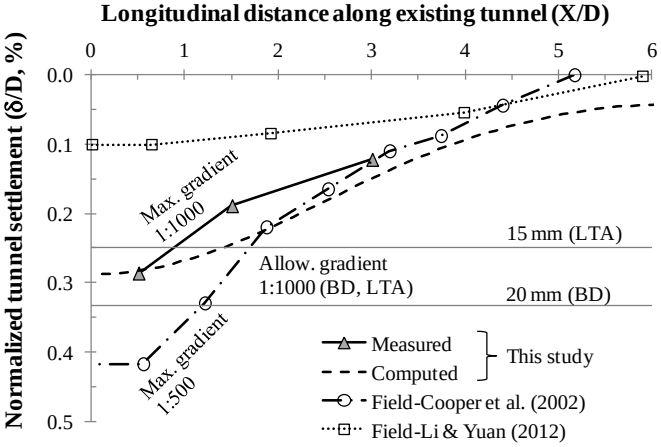

Figure 4. Comparison between measured and computed existing tunnel settlements.

4.2 *Additional strain in the longitudinal direction of the existing tunnel*

Figure 5 shows computed additional strain in the longitudinal direction of the existing tunnel from five key locations; crown, shoulder, springline, knee and invert. The results were illustrated at the end of tunnel excavation. The cracking tensile strain of unreinforced concrete of 150 με (ACI 224R, 2001) is shown as a reference.

By comparing additional strain from the five key locations, the largest additional strain occurred at the crown and invert while the smallest additional strain was induced at the springline. This can be explained by considering differential tunnel settlement (see Fig. 4). At the location directly above the new tunnel, the existing tunnel was bent convex downward. As a result, tensile strain occurred at the lower part of the tunnel (i.e. knee & invert) while the compressive strain was induced at the upper part (i.e. crown and shoulder). In this study, the inflection point was located at a distance between 2 and 2.5D from the centerline of the new tunnel.

Along the invert up to an offset distance of 1D from the new tunnel centerline, the maximum tensile strain of about 200 με exceeded cracking tensile strain of 150 με. It suggested that cracks due to tensile strain may be induced.

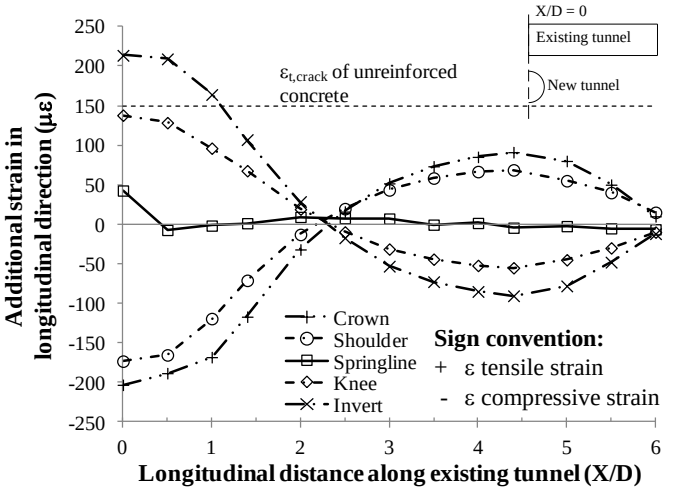

Figure 5. Computed additional strain in longitudinal direction of the existing tunnel.

4.3 *Additional shear stress on tunnel lining*

Figure 6 shows computed additional shear stress along the longitudinal direction of the existing tunnel at the end of tunnel excavation.

The maximum computed additional shear stress occurred along the springline while the additional shear stress along the crown and invert was the smallest. An analogy between shear stress in thin circular tube and computed additional shear stress in this study may be drawn. The maximum shear stress in thin circular tube occurs along the neutral axis and the maximum shear stress is about two times of the mean shear stress in the cross section (Gere, 2001).

The computed additional shear stress was compared with the allowable shear stress. At a given concrete compressive strength (f'_c) of 50 MPa and a reduction factor of 0.55, the allowable shear stress was estimated to be 660 kN/m^2 (ACI 318M, 2011). By comparing with the allowable shear stress, the maximum additional shear stress along the springline (i.e. about 900 kN/m^2) and knee between a distance of X/D = 1 and X/D = 2 exceeded the allowable shear stress. Noted that the location of maximum additional shear stress occurred where the slope of longitudinal additional strain was the steepest (refers to Fig. 5).

Liu (1990; cited by Liao et al., 2008) reported a case study of tunnel differential settlement in Shanghai. Diagonal cracks were observed on the tunnel lining between the location of maximum tunnel settlement and the inflection point of the tunnel. It is il-

lustrated in this study that the additional shear stress can cause cracks along the springline at an offset distance between 1D and 2D from the new tunnel centerline.

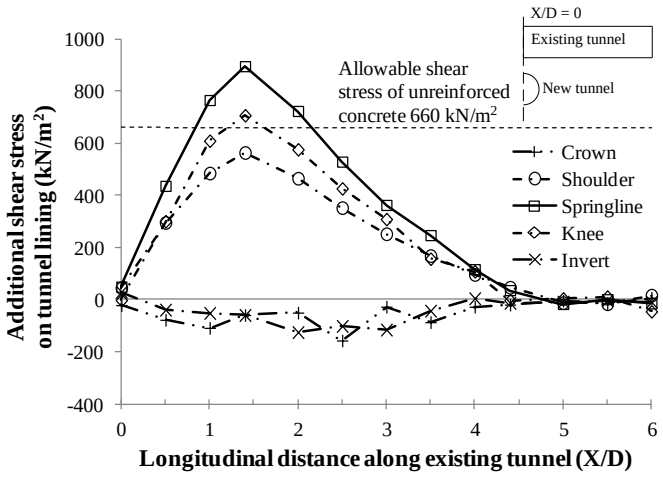

Figure 6. Computed additional shear stress in longitudinal direction of the existing tunnel.

4.4 *Additional strain in the transverse direction of the existing tunnel*

Figure 7 shows comparison of measured and computed additional strain in the transverse direction of the existing tunnel. The results were illustrated when the tunnel face was 0.9D away from the new tunnel centerline (i.e. Y/D = -0.9) and at the end of tunnel advancement (i.e. Y/D = 1.5). Positive and negative additional strain (ε_t) denotes the tensile strain is induced at the outer face and the inner face of the tunnel lining, respectively.

The measured results illustrated that additional tensile strain induced at the inner face of the tunnel lining at the crown and inward. At both springlines, the additional tensile strain induced at the outer face of the tunnel lining. By considering additional strain from crown, both springlines and invert, the existing tunnel was compressed vertically. The maximum measured additional tensile strain of about 50 με occurred at the outer face of both springlines and at the inner face of the invert.

The maximum measured additional strain was still within the cracking tensile strain of 150 με (ACI 224R, 2001). However, if the strain induced during construction of the existing tunnel was large, an increase of strain may still cause serviceability problems to the existing tunnel. Especially, in this case, the existing tunnel was initially vertically compressed due to vertical stress larger than horizontal stress (i.e. $K_0 < 1$).

The computed results show that, additional tensile strain at the crown and both springlines occurred at the outer face of the tunnel lining. At the invert, additional tensile strain was induced at the inner face of the tunnel lining. Maximum computed additional strain at the left springline of about 90 με occurred during the tunnel advancement and decreased at the end of tunnel advancement.

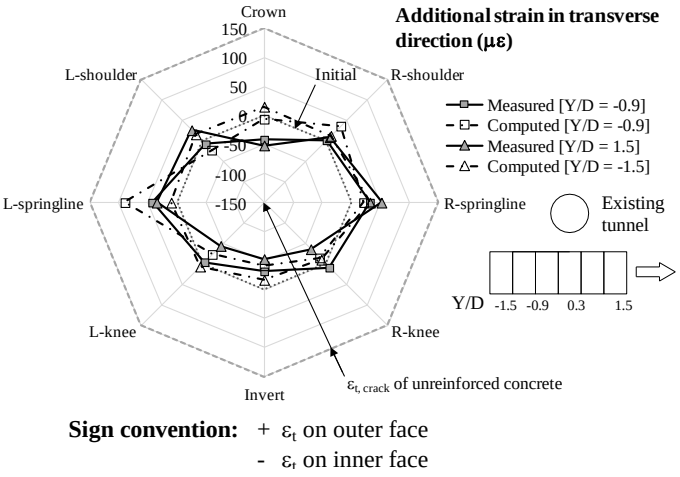

Figure 7. Comparison between measured and computed additional strain in transverse direction of the existing tunnel.

5 CONCLUSIONS

Based on three-dimensional centrifuge model test and numerical back-analysis, the following conclusions may be drawn:

1. Due to a new tunnel excavation perpendicularly crossing underneath, the existing tunnel experienced a large tunnel settlement of about 18 mm (i.e. 0.3% D), which is larger than the allowable limit of 15mm set by LTA (2000).
2. As expected, maximum back-analyzed extra longitudinal tensile strain (i.e. about 200 με) of the existing tunnel occurred along the invert at the location directly above the new tunnel. This additional tensile strain is larger than cracking tensile strain (150με) of unreinforced concrete reported by ACI (2001).
3. Back-analyzed additional maximum shear stress (i.e. 900 kN/m^2) in longitudinal direction of the existing tunnel is larger than the allowable shear stress of 660 kN/m^2 (ACI, 2011) at the springline and knee.
4. Back-analyzed additional maximum tensile strain in transverse direction of the existing tunnel occurs at the left springline. This back-analyzed additional strain is about 90 με, which overpredicted measured additional tensile strain of 50 με.

6 ACKNOWLEDGEMENTS

The authors would like to acknowledge the financial support provided by the General Research Fund 617410 from the Research Grants Council of the HKSAR.

7 REFERENCES

American Concrete Institute. (2001). *Control of Cracking in Concrete Structures* (ACI 224R-01). M.I.

American Concrete Institute. (2011). *Building Code Requirements for Structural Concrete and Commentary* (ACI 318M-11). M.I.

Brinkgreve, R. B. J., Engin, E. & Swolfs, W. M. (2012). PLAXIS 3D 2012 *User manual*. Plaxis bv, Delft.

Building Department (2009). *Practice Note for Authorized Persons APP-24*. Technical notes for guidance in assessing the effects of civil engineering construction / building development on railway structures and operations. Building department of the government of HKSAR.

Cooper, M. L., Chapman, D. N., Rogers, C. D. F. & Chan, A. H. C. (2002). Movements in the Piccadilly Line tunnels due to the Heathrow Express construction. *Géotechnique*, 52(4): 243-257.

Garnier, J. and Coauthors. (2007). Catalogue of scaling laws and similitude questions in geotechnical centrifuge modelling. *IJPMG-International J. Physical Modelling in Geotechnics* 3, 1-23

Gere, J. M. (2001). *Mechanics of materials*. Brooks/Cole Publishing Company, p 440-441

Gudehus, G. (1996). A comprehensive constitutive equation for granular materials. *Soils and foundations*, 36(1): 1-12.

Herle, I. & Gudehus, G. (1999). Determination of parameters of a hypoplastic constitutive model from properties of grain assemblies. *Mech. of Cohes.-Frict. Mater*. 4: 461-486.

Ishihara K. (1993). Liquefaction and flow failure during earthquakes. *Géotechnique*, 43(3), 351-415.

Kim, S. H., Burd, H. J. & Milligan, G. W. E. (1998). Model testing of closely spaced tunnels in clay. *Géotechnique*, 48(3), 375-388.

Kolymbas, D. (1991) An outline of hypoplasticity, *Archive of Applied Mechanics*, 61: 143-151.

Land Transport Authority (2000). *Code of practice for railway protection*. Development & Building Control Department, Land Transport Authority, Singapore.

Li, X. G. & Yuan, D. J. (2012). Responses of a double-decked metro tunnel to shield driving of twin closely under-crossing tunnels. *Tunn. Undergr. Sp. Technol.*, 28: 18–30.

Liao, S. M., Peng, F. L. & Shen, S. L. (2008). Analysis of shearing effect on tunnel induced by load transfer along longitudinal direction. *Tunn. Undergr. Sp. Technol.*, 23: 421–430.

Liu, H. Y., Small, J. C. & Carter, J. P. & Williams, D. J. (2009). Effects of tunnelling on existing support systems of perpendicularly crossing tunnels. *Computers and Geotechnics* 36, 880–894

Liu, J. H. (1990). *Construction technical manual for municipal underground engineering in soft ground*. Shanghai (in Chinese).

Ng, C. W. W., Van Laak, P. Tang, W. H., Li, X. S. & Zhang, L. M. (2001). The Hong Kong Geotechnical Centrifuge. *Proc. 3rd Int. Conf. Soft Soil Engineering*, Dec., Hong Kong. pp. 225-230.

Ng, C. W. W., Van Laak, P. A., Zhang, L. M., Tang, W. H., Zong, G. H., Wang, Z. L., Xu, G. M. & Liu, S. H. (2002). Development of a four-axis robotic manipulator for centrifuge modeling at HKUST. *Proc. Int. Conf. on Physical Modelling in Geotechnics*, St. John's Newfoundland, Canada, pp. 71-76.

Ng, C. W. W., Boonyarak, T. & Mašín, D. (2013). Three-dimensional centrifuge and numerical modeling of the interaction between perpendicularly crossing tunnels. *Tentatively accepted by Canadian Geotechnical Journal*.

Niemunis, A. & Herle, I. (1997). Hypoplastic model for cohesionless soils with elastic strain range. *Mech. of Cohes.-Frict. Mater.*, 2: 279-299.

von Wolffersdorff, P. A. (1996). A hypoplastic relation for granular materials with a predefined limit state surface. *Mech. of Cohes.-Frict. Mater.*, 1: 251-271.

Wu, W., Bauer, E. & Kolymbas, D. (1996). Hypoplastic constitutive model with critical state for granular materials. *Mechanics of materials*, 23: 45-69.

Vorster, T. E. B., Klar, A., Soga, K. & Mair, R. J. (2005). Estimating the effects of tunneling on existing pipelines. *J. Geotech. Geoenviron. Engng*, 131(11), 1399-1410.

Yamashita, S., Jamiolkowski, M. & Lo Presti, D.C.F. (2000). Stiffness nonlinearity of three sands. *J. Geotech. Geoenviron. Engng*, 126(10): 929-938.